GAMMA-RAY BURSTS: CURRENT OBSERVATIONAL PICTURE

Jay P. Norris
Laboratory for High Energy Astrophysics
NASA/Goddard Space Flight Center
Greenbelt, MD 20706

ABSTRACT

We now know that long (duration > 2 s) gamma-ray burst (GRB) sources lie at distances comparable to the "radius" of the Universe and that they are momentarily the most luminous known objects: several GRBs have now been observed to have associated X-ray, optical, and radio counterparts following power-law decays that fit theoretical expectations for relativistic blastwaves. Three GRBs (and/or their host galaxies) have determined redshifts larger than z = 0.8, and virtually all GRBs with associated optical transients appear to lie in distant galaxies. Spectroscopic analysis of afterglows and modeling of the GRB brightness distribution indicate that GRB sources lie in star-forming regions. The population statistics of GRBs as well as their energetic, spectral, and temporal aspects—also consistent with the cosmological distance scale—are difficult but not impossible to explain via neutron star or neutron star-black hole mergers. The suggested association of smooth, single-pulse GRBs with supernovae in nearby redshift space can only involve an insignificant fraction of the total GRB population; moreover the association is contraindicated by the random sky distribution of single-pulse GRBs. Future observations of GRBs with rapid temporal variations at supra-GeV energies by GLAST, the Gamma-ray Large Area Space Telescope, may provide a unique cosmic experiment for constraining the scale of quantum gravity. Detection of a gravitationally lensed GRB would be evidence of a non-zero value for Λ, the cosmological constant.

1 Introduction: Gamma-Ray Bursts Become Highly Visible

Gamma-Ray Bursts (GRBs) are currently enjoying the best public relations since their discovery 30 years ago. Even Sky and Telescope (February 1998), which reaches a large popular scientific audience, featured a fantastic looking cover picture of the suggested progenitor object moments before the GRB explosion. The object which looks like a crackling bowling pin, frozen in time, represents the merger of a neutron-star (NS) binary. Of course the ends of the bowling pin would be rotating at a sizable fraction of the speed of light during the final moments before coalescence. The feature article,[1] appearing one year after the discovery of the first X-ray and optical counterparts to a GRB, concerned the gigantic energy output of GRBs and the theoretical burst of cosmic rays which would follow the electromagnetic (EM) radiation of the GRB in a matter of days. Since the sources of GRBs (at least those of the "long" duration variety) lie at cosmological distances—billions of light-years from our Galaxy—GRBs must be luminous in the extreme. The rate of detected GRBs in the Universe (~ 10^{11} galaxies) —a few per day—translates into ~ one GRB per galaxy per ~ 10^7 years. The total rate would be much higher if the radiation pattern were strongly beamed into a small solid angle: only a small fraction of GRBs would then be detected by Earth observers. Thus, every two rotations of the Sun about the Galactic Center (a half billion years), a GRB would be close enough (~ 1 kiloparsec) for the accompanying cosmic ray burst to annihilate all life on Earth. This is just one of several recent cosmological theories which might provide a sufficiently large energy release to power a GRB.[2] We shall also examine the recent putative connection between type Ic supernovae (SNe) and GRBs, and find that only a very small fraction of GRBs can be connected with SNe.

Observations of NS binaries have already provided interesting tests of physical theory. Table 1 lists several confirmed and suspected NS systems, along with their distances from Earth, rotational periods, and orbital decay times. Included is the famous Hulse-Taylor binary pulsar, which provided the first quantitative evidence for gravitational radiation—energy derived from orbital decay. The distance column is relevant for the GRB/cosmic-ray burst extinction theory, but the decay, or coalescence, timescale provides an astrophysical constraint: When the components of the binary each go supernova, a large velocity kick, ~ 10^3 km s^{-1}, can be imparted to the system. Assuming coalescence timescales of 0.1 – 10 Gyr (still comparable to the age of the Universe), we would look to find at least some of these systems ~ 100 kpc – 10 Mpc outside their parent galaxies. Note however, the systems listed in Table 1 are those we have detected; systems with much shorter decay timescales are much less likely to be discovered before coalescence.

The central questions of source progenitor population and their distribution in redshift, as well as the mechanisms for generation of γ-radiation and the presumed beaming into a narrow solid angle (probably completely distinct from processes governing the counterpart afterglows), all will be constrained—some in ways we do not yet apprehend—not only by evidence from afterglows, but also from the extrinsic characteristics of GRBs and their spectral/temporal behavior.

Table 1: Pairs of Neutron Stars in Our Galaxy

Name	Distance (kiloparsecs)	Period (hours)	Decay Time (10^9 years)
PSR B1534+12	0.5	10.1	2.73
PSR B1913+16 [1]	7.3	7.75	0.30
PSR B2127+11C [2]	10.6	8.05	0.22
PSR B2303+46 [3]	2.3	296	4000
PSR J1518+4904 [3]	0.7	207	2400

[1] Hulse-Taylor pulsar (first direct evidence for gravitational radiation)

[2] In Globular Cluster M13

[3] Suspected binary neutron stars – masses not firmly established

The picture of GRBs at gamma-ray energies as revealed by current instruments on the Compton Gamma Ray Observatory is reviewed in Section 2. We then proceed to examine some more definitively derived constraints imposed by the recent detections at longer wavelengths in Section 3. The apparent association of at least one GRB with an unusual SN is critiqued in Section 4. Section 5 describes two future measurements: a constraint on the energy scale of quantum gravity, using GRBs detected by GLAST; and a constraint on Λ via detection of gravitationally lensed GRBs.

2 GRB Extrinsic Characteristics and GRBs Themselves

2.1 The Distance Scale: Isotropy and the Brightness Distribution

Prior to the discovery of GRB counterparts at longer wavelengths, the extrinsic characteristics of GRBs were endlessly debated, within a milieu of few definitive clues, and mostly under the assumption that GRBs were galactic in origin. The most important extrinsic descriptor — the GRB distribution in space—was originally unconstrained, since the first small GRB detectors were not sensitive enough to sample the entire population. Progressively less oblate spatial distributions (our Galaxy's disk – very much oblate; the Oort Cloud—slightly flattened; our Galaxy's putative "extended halo" —possibly in a common envelope with our sister galaxy, Andromeda) were eliminated as BATSE on the Compton Gamma Ray Observatory detected more and more GRBs, which appeared at random positions on the sky. This isotropic celestial distribution, combined with the fact that BATSE does not detect enough dim bursts compared to the expectation for a homogeneous Euclidean space — indicating that the edge of the spatial distribution is now probed—strongly suggested that GRB sources lie at cosmological distances. All other extrinsic distributions corroborated this appearance, and even before the discovery of counterparts, predicted that GRB sources should lie at redshifts z ~ unity and higher. One distance scale that was never suggested by the data—the "Supergalactic Plane" out to a few times the Virgo cluster distance, ~ 100 Mpc—is now claimed by some investigators as the distance scale for a small subset of GRBs associated with SNe of type Ib/Ic. There is now some evidence against this SNe/GRB connection (see Section 4).

The power outputs from GRBs were then estimable, assuming their cosmological origin. If the power in gamma rays that we observe from the more luminous GRBs is being radiated isotropically, then their instantaneous luminosities, ~ 10^{53} ergs s^{-1} ~ 10^{19} solar luminosities ~ 10^{9} L_* galaxies, would be a few percent of the Universe's power output. If GRBs had turned out to be in the galactic disc, their power output would have been relatively puny, somewhat less than the peak luminosity of a type II supernova, ~ few × 10^{42} ergs s^{-1}. Total GRB radiated energies, integrated over their (unpredictable) durations of 0.01 – 1000 s, would range up to ~ few × 10^{54} ergs, again assuming the unlikely isotropic case.

The web page "www.batse.msfc.nasa.gov" shows the BATSE sky map for the accumulated sample of seven plus years. Occasionally, articles appear suggesting that some subset of GRBs is distributed anisotropically. Indeed, since this map shows individual detections and therefore is necessarily uncorrected for exposure, the equatorial plane is barely perceptible as a zone of slight avoidance. When corrected for exposure with respect to any arbitrary plane, the dipole and quadrupole moments are consistent with isotropy for many subsets of GRBs.[3]

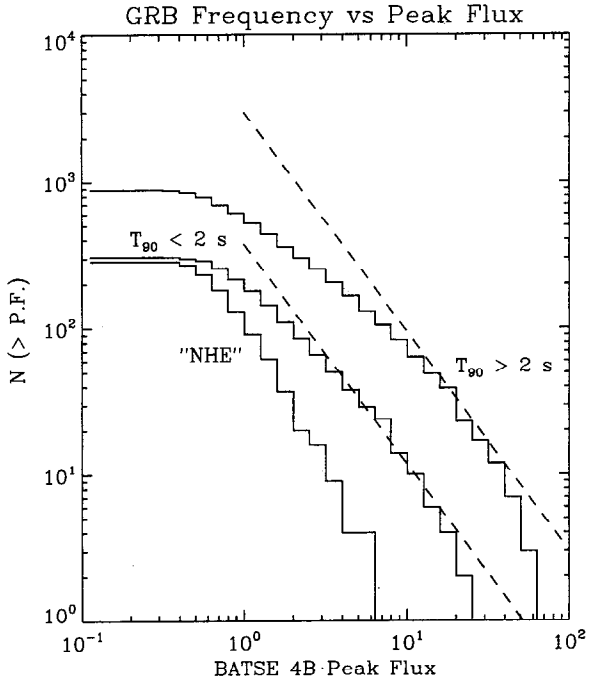

Fig. 1 – GRB brightness distributions for long and short bursts (duration break point at 2 s), and bursts with no high-energy emission ("NHE"), above 300 keV. Dashed lines are -3/2 power laws, which would be expected for uniform homogeneous distributions. Above a peak flux of ~ 1 photon cm^{-2} s^{-1} (50 – 300 keV), BATSE detection efficiency is nearly complete.

Figure 1 shows the much discussed and modeled Log N(umber) – Log P(eak) F(lux) relation for GRBs, also known as the brightness or size distribution. The number of GRBs with PF greater than the abscissa value is plotted on the ordinate. Suppose that GRBs uniformly filled a Euclidean space; then from the simple consideration of three-space, their

brightness distribution would follow a -3/2 power law. The two dashed lines are -3/2 power laws. Shown separately are distributions for long ($T_{90} > 2$ s) and short bursts ($T_{90} < 2$ s); see section 2.4 for a discussion of GRB durations. T_{90} is the interval between the times to accumulate 5% and 95% of the total counts in a GRB. Clearly the long bursts depart more markedly on the dim end from the -3/2 power law, suggesting that we see through more nearly to the edge of their spatial distribution than we do for the short bursts. Said differently, short bursts would appear to be dimmer and not sampled as deeply in redshift space. This is significant, since we have yet to see an X-ray, optical, or radio counterpart for a short burst (the GRB instrument on the BeppoSAX satellite—which has signaled the alert for almost all GRB counterparts so far—does not trigger on short bursts). So short bursts could still be galactic. But, short and long bursts separately have isotropic sky distributions.

The third curve labeled "NHE" (No High Energy) is the brightness distribution for long bursts that have no significant emission above ~ 300 keV. Because of its steeper, nearly -3/2 slope, this subsample has been claimed to be in nearer redshift space, and less luminous because they are supposedly not beamed directly towards Earth.[4] This would constitute the main observational evidence for beaming. However, the apparent NHE class—that is, the approximate slope and normalization of the NHE curve in Figure 1—can be synthetically realized by equalizing the signal-to-noise levels (s/n) of bright bursts (practically all of which have HE emission) to successively dimmer steps in the log N – log PF, and redshifting their spectra (dimmer bursts, presumably at larger redshifts, have softer energy spectra). In this explanation, the steepness of the NHE curve then is due to the combined rapid onset of dimmer and "redder" bursts at lower PF —essentially a brightness bias.[5]

Careers have been spent modeling the GRB brightness distribution, including such extrinsic effects as cosmological time dilation and rate-density evolution with cosmic time; and effects like a GRB luminosity distribution, which may also depend on cosmic time; while also attempting to account for such instrumental effects as incomplete sampling on the dim end and dependence on spectral response. Clearly, we do not presently know enough about GRBs' intrinsic attributes and extrinsic distributions to hope for these efforts to be entirely successful, but we will know enough soon, after accumulation of a sufficient number of redshifts (and therefore luminosities) from counterparts that will calibrate the brightness distribution. The current wisdom in one camp is that the GRB rate-density follows that of star formation,[6,7] which apparently peaked near redshift epoch $z \sim 1.25 - 1.5$, and then declined to the present time. But other modelers[8] claim that a constant GRB rate-density is equally acceptable. Models including luminosity distributions are more realistic (but a broad luminosity range may not be needed) and are consistent with the peak fluxes and redshifts of GRBs 970508, 971214, and 980703 (Ref. 9). It may also be judicious to consider the log N – log PF for long and short bursts separately.[10]

For the cosmological distance scale, it is easy to understand qualitatively why the dim end of the GRB brightness distribution should depart from a -3/2 power law: assume a constant number of GRBs per year, per Mpc^3 everywhere in the Universe. Then two effects diminish the observed number of dim bursts on Earth. First, time dilation makes the "per year" longer for the observer, and second, gravitational lensing of distant volumes by the nearby matter distribution makes the "per Mpc^3" appear larger.

2.2 Cosmological Time Dilation and Spectral Redshift

Before the modern era of counterparts, two additional pieces of evidence supported the cosmology camp's position. (The incredible energetics required of nature was the primary obstacle for the cosmological distance scale, but that is manifestly no longer a problem for nature.) Cosmological time dilation (TD) comes into play not only in log N – log PF as part of the rate-density consideration, but also for the innards of bursts: pulse widths, intervals between pulses, and overall durations. Since GRBs are immensely varied in temporal appearance, there is ample opportunity to measure these timescales. However, measurement difficulties ensue since the dynamic ranges of GRB durations and pulse widths are large. Also, brightness bias and instrument trig gering effects enter the game (GRB monitors usually are half asleep, waiting in low temporal resolution mode for a GRB to occur; then the instrument switches to higher time resolution modes to better record the fast time structure).

We have measured the relative, average widths of dimmer bursts (presumably more distant) compared to those of the brightest bursts (presumably closer) by a variety of methods. All our TD measures include a preparatory step which approximately equalizes the s/n levels of all burst time profiles to that of the dimmest bursts in the sample.[11,12] One particularly "common-sense" method is to group bursts by PF, then within a group, bring the time profiles into temporal registration with the highest peak in each burst positioned at t_0. Estimating the peak time in an unbiased manner is not necessarily straightforward for the artificially dimmed bursts, but is facilitated by a wavelet "denoising" approach. One then measures, e.g., the FWHM of the average profile for each peak-flux grouping and compares these widths with that of the brightest group. This is the observed time-dilation factor (TDF), and would be equal to $(1 + z)/(1 + z_{brightest})$, where z is the average redshift for a given peak-flux group, except that some corrections need to be estimated and applied.

Figure 2 shows the redshift-corrected "peak-aligned" TD measure for ten peak-flux groups from the long burst ($T_{90} > 2$ s) sample only. There are ~ 92 bursts per group. PF is in the standard units for BATSE, photons cm^{-2} s^{-1} (50 – 300 keV). The bootstrap error sizes are mostly due to sample variations (varied temporal appearance, burst to burst), rather than counting statistics. When the brightest group is subdivided further, no significant differences in TDFs result. We have constructed many variants on this sort of TD measure and others (e.g., durations)—varying thresholds, energy ranges, denoising parameters, etc.—and the basic results are always significant and approximately similar: the observed, relative TDF between the brightest and dimmest BATSE bursts is ~ 2. Other investigators report similar results.[13,14,15]

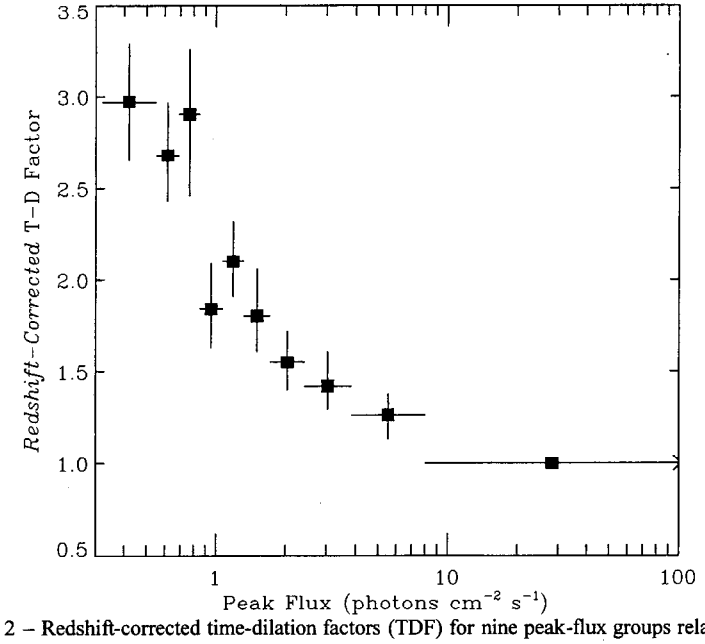

Fig. 2 – Redshift-corrected time-dilation factors (TDF) for nine peak-flux groups relative to the brightest group, for the peak-aligned average profile method.[11,15] There are ~ 92 bursts per group. TDF measures for dimmest three groups utilize only the decaying portion of average profile in attempt to estimate corrections for less than 100% detection efficiency of slowly rising, dim bursts.

At least two correction factors need to be applied to the observed TDFs to realize measures appropriate for comparison with other observables (e.g., log N – log PF). First, because burst temporal structures are intrinsically shorter at higher energy, those portions of the dimmer bursts' profiles that are redshifted into the BATSE detectors' energy band will be narrower than if we were observing the bursts in their comoving frame.[16] We estimate corrections for this complication by s/n equalizing, redshifting, and time-dilating—on a trial grid of TDFs—the bright burst sample to each dimmer sample in succession. Second, BATSE's on-board burst trigger algorithm is "causal": it samples the background for ~ 17 s, then asks if there is a significant (~ 5.5 σ) fluctuation in a 64-ms, 256-ms, or 1024-ms bin succeeding the 17-s integration, in any two of its eight identical detectors (see the web page "cossc.gsfc.nasa.gov/cossc/cossc.html" for descriptions of the Compton GRO instruments and data archive). Thus for dim bursts that rise slowly, the comparison is between a background level and not-so-different levels for the test bins; therefore, BATSE tends to miss slow, dim risers[17]—but not slow, dim decayers, unless they are also slow risers. For PF > 1. photon cm^{-2} s^{-1}, BATSE sampling is ~ 98% complete. For the three dimmer peak-flux groups in Figure 2 we estimated the TDFs by using only the decaying portion of the average time profiles.

The TDF measures plotted in Figure 2 are then an estimate of $(1 + z)/(1 + z_{bright})$, ostensibly with instrumental and redshift effects removed.[18] The dimmest bursts' average profiles are ~ factor of three wider than those of the brightest group. The TDF relation can be combined with the log N – log PF relation to constrain the distribution of GRBs within different model Universes.[8] Results indicate that redshifts of the dimmest bursts (PF ~ 0.1 photon cm^{-2} s^{-1}) detected by BATSE may be as high as $z \sim 5 - 8$. For comparison, the BATSE PFs are ≈ 1.2, 2.3, and 2.6 for the three bursts with associated redshifts $z = 0.835$, 3.412, and 0.966, respectively. The brightest bursts are factors of 10 – 50 brighter, and are predicted to lie at redshifts of a few tenths, if the constant GRB rate-density hypothesis is more nearly correct. If the GRB rate-density follows the star formation rate, then the sources would lie at redshifts of order unity, in which case a broad luminosity distribution may be obtained.

To appreciate the analogous study of burst spectra as a function of PF, we first compare the spectra of high-energy transients in general. From Figure 3, a theorist's $\nu \bullet f(\nu)$ spectral plot, we see that the most intense GRBs are, far and away, brighter and spectrally harder than the most intense X-ray bursters and black-hole binaries, whose spectra usually peter out below ~ 100 keV. The spectra of Soft Gamma Repeaters[19] peak at ~ 10 – 20 keV and disappear above ~ 200 keV. GRB spectra are routinely even harder than the Crab (pulsar +

nebula) power-law spectrum, and have been mapped to EGRET energies, ~ 20 GeV. The spectral peak in $\nu \bullet f(\nu)$ provides a break in the otherwise featureless spectra, with which to measure relative redshift of the sources. Redshift is time dilation of the EM radiation itself. Mallozzi and colleagues performed the analysis,[20] utilizing a sample of long and short bursts, down to a PF ~ 1 photon cm^{-2} s^{-1}, where BATSE detection is nearly complete. From their Figure 1b, a plot of E_{peak} vs. PF, we see that dimmer bursts have progressively lower average $\nu \bullet f(\nu)$ measures, consistent with time-dilation results.

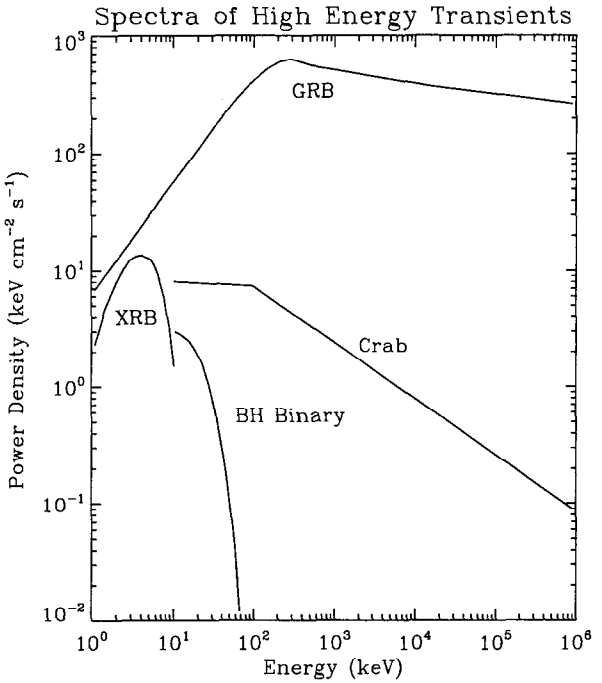

Fig. 3 – Canonical spectra ($\nu \bullet f[\nu]$) of high-energy transients: Gamma-Ray Bursts, X-Ray Binaries, Black Hole Binaries, and the Crab.

2.3 Summary, GRB Extrinsic Characteristics

This much was clear for long bursts, before the detection of counterparts: isotropy of the GRB celestial distribution, the deficit of dim bursts in the log N – log PF, time-dilation and $\nu \bullet f(\nu)$ trends with PF were mutually consistent with the cosmological distance scale hypothesis. None of these indicators individually, nor all combined, proved anything, given that subclasses of GRBs with different distributions could be invoked in models. There are still reasons to entertain possible subclasses.

For example, the distance scale for short bursts has not been established definitively. Short bursts' localizations by themselves are isotropically distributed, as are those of long bursts. But the log N – log PF relation for short bursts does not indicate a definitive deficit at low peak fluxes, since the leveling off on the dim end is more attributable to BATSE detection efficiency: some short bursts are so short that they do not fill the shortest trigger accumulation bin (64 ms). To my knowledge, no one has troubled to model their log N – log PF, probably because of the more severe detection completeness problem. Moreover, short bursts may not be sampled sufficiently deeply in redshift space to manifest curvature, thus modeling may not provide robust constraints given measurement uncertainties.

Some work on time dilation of short burst profiles has been reported.[13] Our work on short bursts does not reveal acceptably stable results as the sample enlarges, or as adjustable parameters are varied. The whole treatment is more difficult: the profiles are so short, containing little information; the definition of peak flux on short timescales is more arbitrary than for long bursts; and unbiased time-dilation measures are difficult to construct and calibrate. The optimum BATSE data type for short bursts, time-tagged two μs photon data, is of limited use due to its 32K maximum event buffer size, which effectively windows the burst record, such that the start and stop times depend on burst brightness. The $\nu \bullet f(\nu)$ vs. PF relation for short bursts shows a barely significant trend (R. Mallozzi, private comm.). Worst for short bursts, BeppoSAX has not detected any, and so there are no X-ray or optical counterparts to go chase, so far.

2.4 GRB Duration Distribution

The brightness distributions for short and long bursts might suggest that they are truly different groups. In fact, their spectral distributions are similar and overlapping, with short bursts tending to be slightly harder. Of course the defining difference is temporal: the logarithmic duration distribution is clearly bimodal, with maxima near 25 s and 300 – 500 ms

(Ref. 21). Distributions for two different duration measures are shown in Figure 4. The dashed histogram is the BATSE team's measurements of the original time profiles for th e "4B" catalog.[22] The solid histogram is our brightness-independent measure, which tends to yield shorter durations for the bright bursts, whose decaying tails are lost upon equalization of s/n levels (analysis as in Ref. 12, using a larger sample here). We measure durations at 64-ms resolution, whereas the BATSE team makes use of the time-tagged event data with two μs

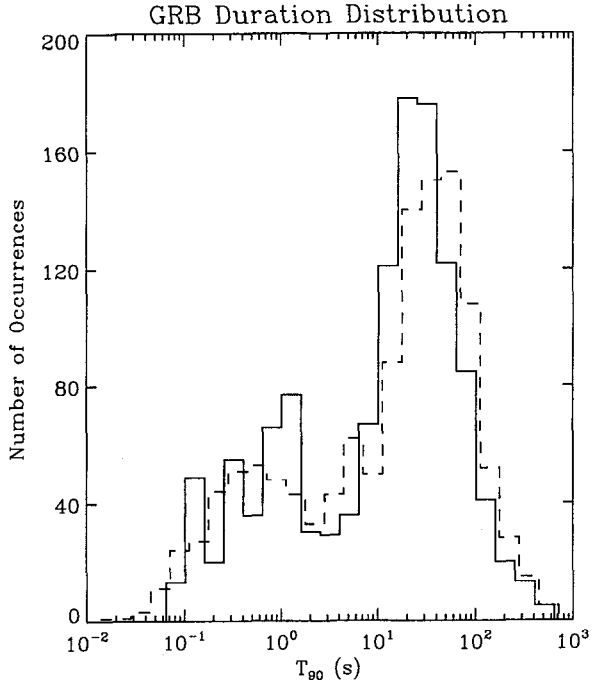

Fig. 4 – GRB duration distributions measured by two different methods (see text). The dashed histogram is derived from data in the BATSE 4B catalog. The solid histogram follows the noise equalization method of Ref. 12, but with a larger sample. T_{90} is the interval between the times to accumulate 5% and 95% of the total counts.

resolution; therefore, their characterization of the short end of the distribution is smoother and of higher fidelity. The valley near 2 – 3 s has been significant since the pre-BATSE era. A few physical explanations for the duration bimodality have been proposed. Recently, Yi and Blackman[23] proposed that the two classes correspond to accretion-induced collapse of white dwarfs to millisecond pulsars formed spinning above or below a gravitationally unstable limit, with the collapse followed by either gravitational radiation (short bursts) or electromagnetic dipole radiation (long bursts), respectively. The gravitational radiation from white dwarf collapse to pulsar may be rarely detectable for the very nearest short bursts.[23,24] NS binary coalescence may be detectable by LIGO out to a few times the Virgo cluster distance (tens of Mpc), but the event rate would be low, perhaps one event per decade.[25]

2.5 GRB Temporal Profiles

Since my interest concentrates on characterization of the widely varied temporal behavior of GRBs, I will avoid dwelling on this aspect. For the reader who would undertake serious temporal investigations, the most expeditious route to the BATSE data is through the GRO guest investigator web pages.[26] Here, discussion of two time profiles will suffice. Figure 5 illustrates a very short burst, GRB 930131, famous for its wavefront passing by the Earth during Superbowl XXXII. The triangles represent individual photons detected by the EGRET spark chamber; the histogram is the BATSE light curve, at energies > 25 keV. Because the spark chamber deadtime is ~ 100 ms per photon, the actual evolution at EGRET energies (> 30 MeV) is not measured during the intense ~ 200 ms spike-like pulse. Such fast, narrow GRBs might afford a natural experiment for probing the quantum gravity energy scale since photon arrival times may be dispersed as a function of energy (see section 5).

Visually, short bursts appear to have one or just a few emission episodes, or "pulse structures." Often a short GRB consists of a solitary pulse. However amongst short bursts can be found examples with many pulses and pulse structures, and these appear self-similar to the long bursts. The definition of pulses in short bursts is limited by statistics. Perhaps short bursts as a group would appear even more similar to long bursts if short bursts were observed with much larger detectors—then the pulse fluctuations would be as well-defined as for long bursts. Figure 2 of Ref. 27 illustrates GRB 940217, a complex burst from the long end of the duration distribution. This intense burst, also detected by EGRET, is famous for a 20 GeV photon which arrived 5000 s after the burst faded at lower energies, as detected by BATSE and Ulysses.

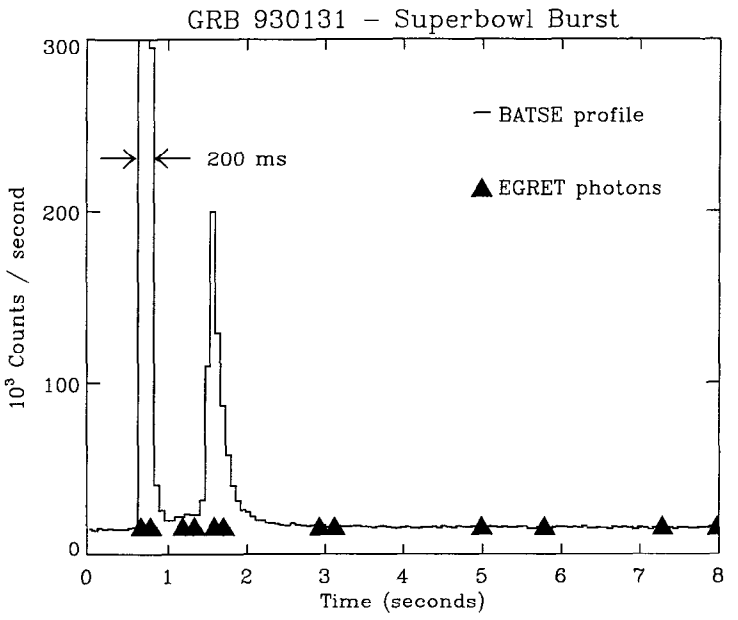

Fig. 5 – GRB 930131 (whose wavefront passed by the Earth during Superbowl XXXII) as detected by BATSE and EGRET. Vertical axis is truncated: maximum BATSE count rate was $> 7 \times 10^5$ s^{-1} , and limited by deadtime effects. EGRET spark chamber deadtime per event is ~ 100 ms. Thus neither instrument recorded actual fluxes during the initial intense spike.

Short and long bursts are similar in two other respects. Both tend to exhibit hard -to-soft spectral evolution, within a pulse and across the entire duration of an event: Pulses tend to be longer and their onsets later at lower energies, and bursts tend to be longer at lower energies. However, both groups exhibit the "asymmetry pulse paradigm": the more asymmetric a pulse, the wider it is, with lower energies peaking at later times. Conversely, in nearly symmetric pulses, the peaks are aligned across energy bands.[28,29]

Since the radiation mechanisms of GRBs may be completely separate from processes governing their counterpart afterglows, the temporal/spectral development at gamma-ray energies will remain central to eventual understanding. Recent temporal analysis work employing objective algorithms for the determination of the number of pulses in a burst, as well as pulse rise and decay times, has been done by Scargle[30], using a newly formulated "Bayesian Block" approach to estimate position s of change-points —where the mean changes significantly. Constraints that GRB time profiles impose on internal vs external shock models, via considerations of kinematics of the expanding emission front, have been expounded by Fenimore and co-workers.[31]

3. GRB Counterparts at Longer Wavelengths

3.1 Discoveries of GRB Counterparts and High Redshifts

On February 28, 1997, the gamma-ray burst community was surprised by the breakthrough discovery of an X-ray counterpart to GRB 970228, detected by the BeppoSAX GRB monitor and the narrower field X-ray instruments. The evidence from two observations, separated by three days, revealed the appearance and decay of a previously unknown X-ray source consistent with the position of the GRB.[32] Subsequent X-ray detections of GRBs, outnumbering optical detections by about two to one, have established a clear pattern of power-law temporal decays, predicted by Meszaros and Rees as the signature of cosmological fireballs/blastwaves in the aftermath of a GRB.[33]

The X-ray localization accuracy (~ 3 arc minutes) from BeppoSAX's wide field camera was sufficiently refined to allow deep pointed observations with large optical telescopes. The path to The Holy Grail of GRBs was then established by van Paradijs, Sahu, and Galama,[34,35,36] upon observing the X-ray error circle on Mar 1 and Mar 8 with the William Herschel (4.2 m) and Isaac Newton (2.5 m) telescopes, and finding a decaying optical source at visual magnitude ~ 21—extremely faint compared to previous claims of possible archival optical associations with GRBs. Two weeks later the field was observed by HST. The closeup revealed the still-bright GRB counterpart, compared to an extended nebulosity—the host galaxy. Comparison with a second HST observation made on Apr 2 led Caraveo and colleagues[37] to declare that the object had manifested a proper motion of 18 milliarcseconds, and was probably a compact star moving at ~ 250 km s^{-1} at a distance of ~ 100 pc; ~ 0.1 pixel centroiding was claimed, and possible to achieve.

HST observed the transient again in September and one year after the GRB.[38] By September the afterglow had faded considerably. No measurable proper motion had occurred in six months. (The positional analysis problem, as explained by D. Macchetto of the HST Institute, involved delicate subtraction of the underlying galaxy's light, which had a gradient in the direction of the GRB.) HST images revealed details of a foreground galaxy with the faint transient superposed, and other distant galaxies at redshifts of ~ unity, each of angular size ~ 1 arc second. There was the small probability of chance superposition, but with each subsequent optical counterpart to a GRB, evidence of a host has emerged—spatial coincidence, temporal decay pattern, and/or spectral reddening—indicating that the GRB source is embedded in an obscuring region, i.e., galaxian dust and gas. (Note, galaxies at redshifts z ~ 1 and higher tended to be smaller, closer together, and less organized. So whereas it would require less time for a supernova-kicked NS binary to escape from its smaller galaxy with weaker gravitational pull, the binary would soon find itself near another galaxy, at least in projection on the sky. So the question of transient/galaxy association was pertinent with this sample of one, and may still be for some subclass of GRB.)

During Mar 31–Apr 2, 1997, Tonry and colleagues obtained a 5500-s spectrum of the transient with the Keck II 10-m telescope; no obvious emission lines were identified, and no redshift was found.[39] After significant fading (Aug 13, 5.5 months after the GRB), Kulkarni and colleagues[40] performed an 1800-s integration with the Keck II to acquire the spectrum of transient and galaxy; still no strong emission lines were observed, and thus no redshift was obtained. The Holy Grail was missing.

Meanwhile, GRB 970508 was detected by BeppoSAX, and its behavior followed somewhat different patterns. The X-ray temporal decay revealed a significant bump in an otherwise power-law decay, at a delay of ~ 1 – 3 days. This relatively long lasting bump (compared to the GRB duration) contained ~ 25% of the fluence of the X-ray afterglow, and ~ 5% of the total energy released by the GRB. Piro and colleagues[41] suggested that afterglow and gamma rays arise from the same primary process, just on timescales differing by ~ 10^4. Optical flaring occurred nearly simultaneously with the X-ray bump. Fenimore and colleagues[31] used these kinds of temporal features, both during the gamma-ray events and the X-ray afterglows, to argue on a kinematic basis that external shocks could not be the driving radiative mechanism. Internal shocks for the GRB itself are favored on theoretical grounds.

The optical light curve of GRB 970508 showed the brightness remaining practically constant during the first day, and then rising to maximum light (R magnitude ~ 20) before beginning the power-law decay.[42] Near 100 days, hint of a departure from power-law decay appeared. This departure was observed to continue to day ~ 300, and is well-fitted by a power-law plus constant. The temporal fit and the photometric colors implied a small, faint host galaxy of the starburst variety, with ~ 3 kpc diameter.[43] In August 1998, the galaxy was imaged by HST, revealing a small (0.07 arc second) but extended, elliptical object with R magnitude ≈ 25.3 (Ref. 44). And of course, GRB 970508 was the Holy Grail: The light of the transient itself showed an absorption line system and oxygen emission,[45] both with redshift z = 0.835, roughly half the distance back to the start of spacetime.

GRB 970508 was also detected in the radio by Frail and colleagues[46] and revealed the signature of an (initially) adiabatically expanding fireball.[47] The radio signal was first detected at one week delay, at 4.9 and 8.5 GHz. Variations over the succeeding month, and their subsequent quenching, are indications of diffractive scintillation due to the initial small angular size (analogous to stars twinkling as their light passes through the atmosphere) and then expansion to an apparent size of ~ 10^{17} cm (~ 6×10^3 AU), with expansion velocity near the speed of light. The observed behavior at a several-week delay indicates evolution from highly relativistic to sub-relativistic, $\Gamma \sim 2$, as the fireball expands transversely, becoming less beamed and more spherical. Taking into account the probable nonspherical expansion, the implied fireball energy was ~ 2×10^{51} ergs (Refs. 46 and 47).

GRB 971214, the third with an optical counterpart, was imaged by HST on May 7, 1998 (Ref. 48). The transient had faded by then but a faint host galaxy, R magnitude ≈ 25.5, was found at the transient's position. The probability of chance superposition is estimated ~ 10^{-2} – 10^{-3}: ~ 4×10^5 galaxies per degree^2, brighter than 25.5 magnitudes, and the galaxy's apparent radius is ~ 0.35 arc seconds. The index for the afterglow power-law decay was $\alpha \sim 1.4 \pm 0.2$, slightly steeper than those for GRBs 970228 and 970508, with $\alpha \sim 1.1$ and 1.2, respectively.[49] GRB 971214's optical transient was fainter and redder than the previous two, suggesting a dense star-forming environment for the GRB progenitor.

Kulkarni and colleagues[48] determined the redshift of the apparent host galaxy after the GRB faded (a usable spectrum of the transient itself could not be obtained). The galaxy's light revealed a Lyman α emission line (consistent with drop in the blueward continuum, due to intervening hydrogen absorption), at a redshift identical to that of several galaxian absorption lines, species routinely found in high redshift, star-forming galaxies. The measured redshift is z = 3.148, ~ 90% of the distance back to the Big Bang, considerably higher than that for GRB 970508 at z = 0.835. The gamma-ray peak flux of GRB 971214 was ~ 2 × that of GRB 970508. Luminosity goes as $(1 + z)^3$, so GRB 971214 would be ~ 25 × more luminous than GRB 970508— the first observational evidence of a GRB intrinsic luminosity distribution. If the burst emission were isotropic, then the total gamma-ray fluence in the burst would be ~ 3×10^{53} ergs. The GRB lasted about 20 s, so the isotropic

average flux would be ~ 10^{52} ergs s^{-1}. The energy in the optical afterglow is estimated as ~ 2 × 10^{51} ergs, largely independent of beaming considerations, since the fireball expansion is presumed to be subrelativistic and nearly symmetric. And since the afterglow is best understood as an adiabatic phenomenon, a very small fraction of the energy available in the fireball is radiated. This is one energetics basis for the claim[50] that NS-NS or NS-BH mergers come up short, given the likely conversion efficiency to γ's (< few percent) and the available rest mass of the binary, ~ 5 × 10^{33} gm.

3.2 Summary: GRB Counterparts

Table 2 summarizes the nine optical counterparts to GRBs identified through July 1998. Some assumptions about conversions between energy bands and cross-instrument calibrations were necessary. Host galaxy magnitudes for the more recent GRBs are in the process of revision as the optical transients continue to decay. So not all entries are definitive. Variations in the γ/X peak flux ratio and X-ray spectra are taken as evidence of varying amounts of obscuration near the GRB source, indicative of star-forming regions.[51] In each case we have imaging, spectroscopic, and/or light-curve evidence of a host galaxy. The images are very faint extended/elongated smudges, but coincident in position with the optical counterpart. Given precise optical positions, radio counterparts are now routinely detected for a good fraction of GRBs. A third redshift (z = 0.966) for the optical transient associated with GRB 980703 has been obtained. The absorption lines in its spectra also indicate the presence of a star-forming galaxy.[52] Note that GRBs 970508 and 980703 have comparable redshifts, and their gamma-ray peak fluxes differ by a factor of only ~ 2, an indication that the GRB luminosity distribution may not be too broad. However, Fruchter[53] argues that the IR-optical colors for the GRB 980329 transient are best interpreted as absorption due to the Lyman α forest extending to a redshift z ~ 5, implying a luminosity distribution in peak flux greater than 100.

The combined astrometric and spectroscopic evidences indicate that those GRB sources with associated optical counterparts are inside star-forming galaxies. Bloom and colleagues[54] derive a median merger timescale of ~ 10^{8} years, and thus the sites of NS-NS mergers should be in close association with star formation regions, rather than outside host galaxies. Van den Heuvel maintains that many NS-NS binaries may merge on even shorter timescales. His calculation extrapolates from the observed properties of B-emission X-ray binaries, which comprise one neutron star and a massive companion, to arrive at the expected distribution of orbital periods after the second supernova. The result is that ~ 50% of NS - NS binaries may form with sufficiently short orbital periods such that they merge within 10^{7} years, leaving GRB sources well inside star-forming regions in host galaxies.[55] However, optical counterparts have been detected only for the two-thirds of GRBs in which rapid, longer wavelength observation strategies were possible; the other third may be those where the progenitor long ago escaped the host. We would hypothesize that optical emission requires a dense environment and so is not generated in those cases.

Table 2: Gamma-Ray Bursts with Optical Counterparts.

GRB	Peak Fluxes [7]					Host Galaxy	
	γ-ray [1]	X-ray [2]	γ/X Ratio	Optical [3]	Radio [4]	Brightness [5]	z [6]
970228	3.5	2.3	80	20.5	—	24.6	—
970508	1.2	3.0	25	19.8	1.2	25.8	0.835
971214	2.3	2.5	56	21.7	—	25.5	3.412
980326	1.3	4.7	17	21.0	—	25.3	—
980329	13.3	70.0	12	23.6	0.25	~ 29 ?	~ 5 ??
980425	1.1	2.6	26	13.7	49	14.3	0.0085
980519	4.7	2.9	100	20.4	0.1	24.7	—
980613	0.63	0.7	57	22.9	—	24.4	—
980703	2.6	4.0	40	20.1	1.0	23.0	0.966

[1] photon cm^{-2} s^{-1} (50–300 keV); conversion factor, photons to ergs, ≈ 6.15 × 10^{-7}.

[2] ×10^{-8} ergs cm^{-2} s^{-1} (2–10 keV).

[3] R band magnitude.

[4] milli Jansky, at 8.4 GHz (10 GHz for GRB 980425).

[5] R band magnitude, corrected for galactic extinction.

[6] Redshift.

[7] See these two web pages for many current references on GRB afterglows: GRB Coordinates Network notices, used to distribute GRB news rapidly, gcn.gsfc.nasa.gov/gcn/ ; and www.obs.aip.de/~jcg/grbgen.html.

4. SN 1998bw ≡ GRB 980425?

The clearly outstanding burst in Table 2 is GRB 980425 (optical peak flux ~ magnitude 14!!), for which the claimed optical counterpart—an unusual SN of type Ic —is suspect. Figure 6 illustrates the BATSE time profile of this relatively weak, monolithic burst in four energy bands (~ 25–50, 50–100, 100–300, > 300 keV) at 0.5-s resolution, with fits to the lower three energy bands using a single lognormal pulse model. It is probably not remarkable that the burst is not detected above 300 keV, since "no high-energy emission" has been shown to be attributable to brightness bias.[5] The tendency for high energy to lead low energy is obvious. The BeppoSAX Wide Field Camera localized this burst within an error circle ~ 15 arc minutes in diameter. Contained within the circle, and imaged by the Narrow Field Instruments, were two X-ray sources with error circles ~ 2 arc minutes in diameter. One of these sources faded away by the second NFI observation, and that's the last we know of it – was it the true counterpart? Also, an unusual supernova—1998bw—was found adjacent to but consistent with neither X-ray error region. Radio emission from SN 1998bw was also detected, ~ 10 × stronger than that for any other type Ic SN (but only a handful have radio detections), leading investigators to conjecture that the association is not by chance.[56]

To make the connection even more appealing, the extrapolated optical t_0 for the SN is plus or minus a couple days of the GRB. And, an available kinetic energy of few × 10^{52} ergs is suggested from modeling the optical light curve, assuming ejection of 0.7 $M_\odot$ of ^{56}Ni, about 10 × that usually produced in core-collapse-induced SNe[57]. Some SN aficionados are having a field day, going so far as to assert that all GRBs may be associated with unusual SNe, and that we are merely seeing ~ 10^{-3} of the total GRB population: The distant, very luminous GRBs that we detect are beamed at us in a narrow cone, and therefore we see a small fraction of the total, but from a much larger volume. GRB 980425 would be one of the more frequent ones in this large volume, but much closer and therefore visible, and we see a different kind of optical counterpart by virtue of its isotropic, lower intensity emission.[58] The redshift of SN1998bw is z = 0.0085, corresponding to a distance of 38 Mpc, about twice the distance to the Virgo cluster. The chance of finding this kind of SN inside the BeppoSAX WFC error circle is now very small, given the unusual energetics, and the close temporal coincidence. Too small to calculate confidently, or to ignore.

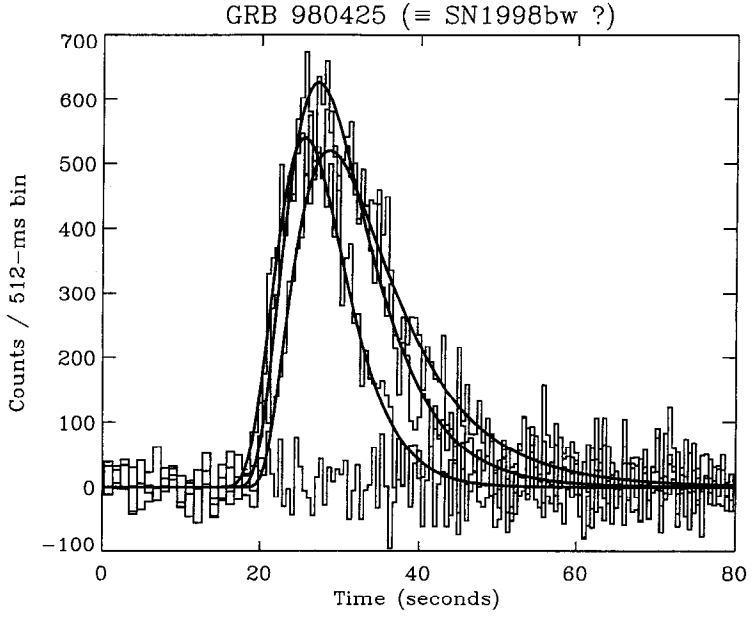

Fig. 6 – BATSE time profiles and lognormal fits for GRB 980425—a relatively weak, smooth, single-pulse burst. The fitted peak occurs progressively earlier at increasing energy (channels 1–3: 25–50, 50–100, 100–300 keV), an example of hard-to-soft spectral evolution in a pulse. The absence of emission above 300 keV is not remarkable, since "no high-energy emission" is likely attributable to brightness bias.[5]

Bloom and colleagues[59] summarize the attributes of SN1998bw and GRB 980425, and come to the conclusion that perhaps ~ 1% of BATSE GRBs could be SN type Ic. The required GRB attributes are a single, broad pulse exhibiting hard-to-soft spectral evolution with longer decay than rise; possibly no high-energy emission; and no X-ray afterglow. The upper limit for any set of GRBs being associated with nearby SNe must be ~ 10%, given isotropy. BATSE's detection limit for type Ic SN is estimated to be ~ 100 Mpc (Ref. 59). The nearby luminous matter distribution to ~ 100 Mpc is highly nonuniform, following a linear feature from the Pegasus to Virgo to Coma clusters—the Supergalactic Plane—the one distance scale never previously demonstrated as a possible home for GRBs.

We visually searched our collection of background-subtracted, noise-equalized (to the peak intensity of GRB 980425) time profiles of long bursts, liberally including in a first-cut sample anything remotely resembling a single-pulse event. In automated passes, we fitted a lognormal pulse model, excluding from further consideration those bursts with poor χ^2 or correlated residuals in channels 1, 2, or 3—considering such to be evidence of more than one pulse. The automated pass largely confirmed our expectations from the visual inspection. We also restricted consideration to those bursts with FWHM within a factor of three of GRB 980425's (4 – 35 s). Thirty-two bursts passed these cuts, and about five of these have "no high-energy emission." Most are dim bursts, and they have a clear resemblance to GRB 980425. Most but not all exhibited hard-to-soft spectral evolution.

For the two sets, with and without high-energy emission, we searched an exhaustive list of 900 SN (most are the more luminous SN type II or type Ia) from the BATSE era. The list is more complete by ~ factor of two during the last two to three years due to heightened interest in high z objects. We found one or two possible SN associations for the NHE + HE set, given the time constraint that the GRB must precede the first SN observation in any case. Correcting for SN detection incompleteness in previous years, we estimated that ~ 5 GRBs could be associated with SN type Ib/Ic.

We were able to find redshifts for two-thirds of the type Ib/Ic SNe, and they are indeed nearby: the redshifts are $z <\sim 0.0175$, i.e., up to roughly twice the distance of SN 1998bw ($z = 0.0085$). Both the nearby SNe and the single-pulse GRBs might be expected to show a preference for the Supergalactic Plane. In Figure 7 the SNe are plotted in the supergalactic coordinate system. The continuous line is the Galactic Plane. Note that 16 of these 21 SNe fall within 30° of the Supergalactic Plane and that they tend to avoid the region near the Galactic Plane (due to obscuration). As expected, the quadrupole moment, $\langle \sin^2 b - 1/3 \rangle$, for the SN distribution with respect to the Supergalactic Plane (b = supergalactic latitude) is significantly oblate at the 2-σ level, $-0.138^{+0.067}_{-0.043}$, where errors are estimated via a bootstrap approach. Figure 8 shows the 32 single-pulse GRBs in the same coordinate system. There appears to be no tendency for any subset of single-pulse GRBs to fall near the Supergalactic Plane. The quadrupole moment for the entire GRB single-pulse set is $-0.003^{+0.05}_{-0.05}$ – not significantly different from zero.

For economy of hypotheses, we suggest that some source population other than nearby SNe generally accounts for the smooth, single-pulse GRBs. We conclude that either the SN1998bw – GRB980425 association is coincidental, or events of this type comprise a very rare and distinct phenomenon.[60]

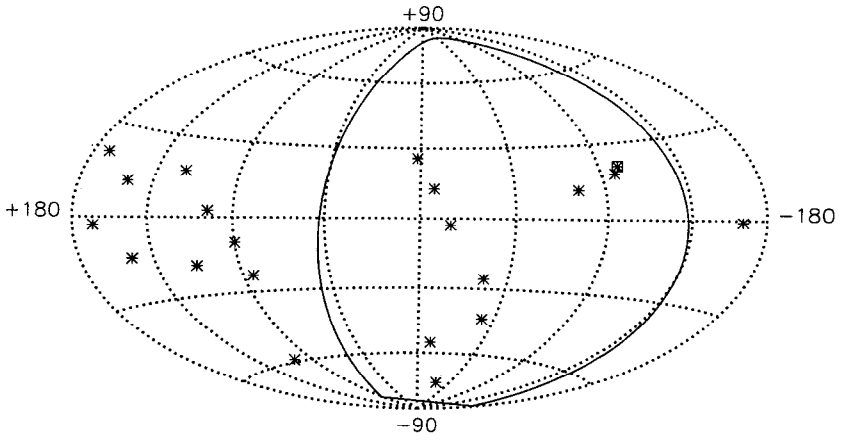

Fig. 7 – The 21 SNe of type Ib or Ic found in the IAUC supernovae catalog, plotted in the supergalactic coordinate system. The continuous line is the Galactic Plane. Sixteen SNe lie within 30° of the Supergalactic Plane. The symbol inside the square indicates SN1998bw. The quadrupole moment for the SN distribution with respect to the Supergalactic Plane is significantly oblate at the 2-σ level, $-0.138^{+0.067}_{-0.043}$.

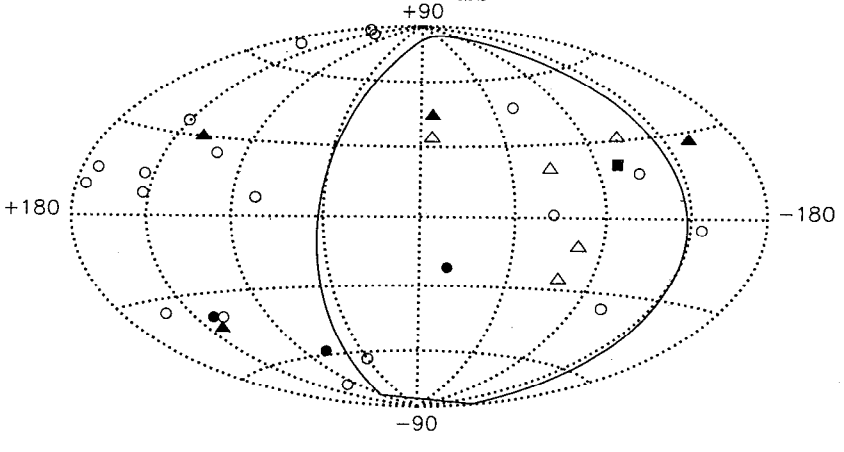

Fig. 8 – The 32 single-pulse GRBs in the supergalactic coordinate system. Circles indicate GRBs with peak > 720 counts s^{-1}; triangles indicate bursts below this threshold—too dim to determine reliably the number of pulses present. Filled (open) symbols are NHE (HE). No subset of single-pulse GRBs shows a tendency to cluster near the Supergalactic Plane.

5. *Future High-Energy GRB Instrument*

GLAST—Gamma-ray Large Area Space Telescope, the next generation high-energy gamma-ray telescope—comprises a pair-production tracker with a hodoscopic calorimeter and a segmented anti-coincidence shield. Using the most powerful particle accelerators in the Universe as cosmic laboratories, GLAST will explore the link between gravitation and quantum physics in the extreme environments of supermassive black holes, neutron stars, and gamma-ray bursts. On cosmological scales, GLAST will explore the era of star formation in the Universe, the physics of dark matter, and the creation and evolution of galaxies. Most important from my parochial point of view is that GLAST will detect GRBs to supra-GeV energies. Recall the Superbowl Burst plotted in Figure 5. Because GLAST will have insignificant deadtime and will be much more sensitive than EGRET, it offers the possibility of probing the quantum gravity scale, E_{QG}: Photon arrival times may be energy dependent, by virtue of dispersion in the vacuum of spacetime, hypothesized to be granular at the Planck scale.[61] Using the very fast, narrow rise features in some bursts, and taking advantage of the high-energy GRB radiation that travels gigaparsecs, we may be able to search for this distance-dependent and energy-dependent effect using GLAST: The brightest ~ 25 GRBs per year should be detectable at energies ~ 100 GeV, with dispersions of ~ 10 ms GeV^{-1} Gpc^{-1}. *Just as important for probing star and galaxy formation in the early Universe, the tracker's* angular resolution will be good enough to localize ~ 100 GRBs per year to better than ~ 10 arc minutes, as shown in Figure 9—sufficiently accurate to enable followups at all longer wavelengths.

Finally, detection of one or two cosmological lenses ("images" separated temporally by months to years) amongst the dimmest, untriggered BATSE bursts would be expected (G. Marani, private comm.) if the cosmological constant $\Lambda \sim 0.6$ and if the GRB rate-density follows that of star formation in the Universe.

Acknowledgments

I am very grateful to Jerry Bonnell and Gabriela Marani for many enlightening conversations and for much help in assembling GRB counterpart flux measurements.

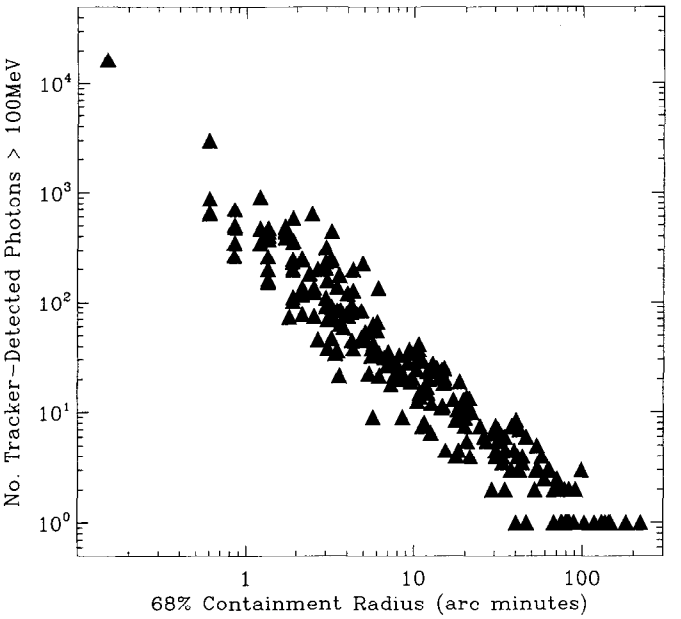

Fig. 9 – Simulated GRB localization accuracy for GLAST's silicon strip tracker: two-dimensional 68% containment angle vs number of detected photons above 100 MeV. The simulation algorithm takes into account measured GRB duration, brightness, and spectral shape distributions, assumes satellite zenith-pointing mode, and utilizes GLAST tracker reconstruction methods. Approximately 100 GRBs per year should be localized to better than *ten arc minutes.*

References

[1] P. J. T. Leonard and J. T. Bonnell, Sky and Telescope, p. 28 (February 1998).

[2] N. J. Shaviv and A. Dar, MNRAS 277, p. 287 (1995).

[3] M. F. Briggs et al., Astrophys. J. 459, p. 40 (1996).

[4] G. N. Pendleton et al., Astrophys. J. 464, p. 606 (1996).

[5] J. T. Bonnell and J. P. Norris, Astrophys. J. (1998) (submitted).

[6] P. Madau, MNRAS 282, p. 1388 (1996).

[7] R. A. M. J. Wijers et al., MNRAS 294, p. L13 (1996).

[8] E. E. Fenimore and J. S. Bloom, Astrophys. J. 453, p. 25 (1995).

[9] M. R. Krumholz et al., Astrophys. J. (1998) (astro-ph/9807117) (submitted).
[10] J. M. Kommers et al., Astrophys. J. (1998) (astro-ph/9809300) (submitted).
[11] J. P. Norris et al., Astrophys. J. 424, p. 540 (1994).
[12] J. T. Bonnell et al., Astrophys. J. 490, p. 79 (1997).
[13] H. Che et al., Astrophys. J. 483, p. L25 (1997).
[14] M. Deng and B. E. Schaefer, Astrophys. J. (1998) (astro-ph/9806010) (submitted).
[15] M. L. Litvak et al., in Gamma-Ray Bursts, AIP 428, p. 176 (1998).
[16] J. P. Norris, AIP 384, p. 13 (1996).
[17] J. M. Kommers et al., Astrophys. J. 491, p. 704 (1997).
[18] J. P. Norris et al., Astrophys. J. (1999) (to be submitted).
[19] C. Kouveliotou et al., Nature 393, p. 235 (1998).
[20] R. S. Mallozzi et al., Astrophys. J. 454, p. 597 (1995).
[21] C. Kouveliotou et al., Astrophys. J. 413, L101 (1993).
[22] C. A. Meegan et al., Current BATSE GRB Catalog: www.batse.msfc.nasa.gov/data/grb/catalog/.
[23] I. Yi and E. G. Blackman, Astrophys. J. 494, p. L163 (1998).
[24] D. Lai and S. L. Shapiro, Astrophys. J. 442, 259 (1995).
[25] C. S. Kochanek and T. Piran, Astrophys. J. 417, L17 (1993).
[26] Compton GRO Guest Investigator Resources (GRB temporal profiles): http://cossc.gsfc.nasa.gov/cossc/batse/4Bcatalog/4b_basic.html.
[27] K. Hurley et al., Nature 372, p. 652 (1994).
[28] J. P. Norris et al., Astrophys. J. 459, p. 393 (1996).
[29] J. P. Norris, Astrophys. Space Sci. 231, p. 95 (1995).
[30] J. D. Scargle, Astrophys. J. (1998) (astro-ph/9711233) (submitted).
[31] E. E. Fenimore et al., Astrophys. J. (1998) (astro-ph/9802200) (submitted).
[32] E. Costa et al., Nature 387, p. 783 (1997).
[33] P. Meszaros and M. J. Rees, Astrophys. J. 476, p. 232 (1997).
[34] J. van Paradijs et al., Nature 386, p. 686 (1997).
[35] K. C. Sahu et al., Nature 387, p. 476 (1997).
[36] T. Galama et al., Nature 387, p. 479 (1997).
[37] P. Caraveo et al., IAU Circ. 6629 (1997).
[38] A. S. Fruchter et al., Astrophys. J. (1998) (astro-ph/9807295) (submitted).
[39] J. L. Tonry et al., IAU Circ. 6620 (1997).
[40] S. R. Kulkarni et al., IAU Circ. 6732 (1997).
[41] L. Piro et al., A&A 331, L41 (1998).
[42] H. Pedersen et al., Astrophys. J. 496, p. 311 (1998).
[43] S. V. Zharikov, V. V. Sokolov, and Yu. V. Baryshev, A&A 337, p. 356 (1998).
[44] J. S. Bloom et al., Astrophys. J. (1998) (astro-ph/9807315) (submitted).
[45] M. R. Metzger et al., Nature 387, p. 878 (1997).
[46] D. A. Frail et al., Nature 389, p. 261 (1997).
[47] E. Waxman, S. R. Kulkarni, and D. A. Frail, Astrophys. J. 497, p. 288 (1997).
[48] S. R. Kulkarni et al., Nature 393, p. 35 (1998).
[49] J. P. Halpern et al., Nature 397, p. 41 (1998).
[50] A. N. Ramaprakesh et al., Nature 393, p. 35 (1998).
[51] A. Owens et al., Astronomy and Astrophys. (1998) (astro-ph/9809356) (submitted).
[52] S. G. Djorgovski et al., Astrophys. J. (1998) (astro-ph/9808188) (submitted).
[53] A. S. Fruchter, Astrophys. J. (1998) (astro-ph/9810224) (submitted).
[54] J. S. Bloom et al., Astrophys. J. (1998) (astro-ph/9805222) (submitted).
[55] E. P. J. van den Heuvel, in X-Ray Binaries and Recycled Pulsars (Kluwer Acad. Publishers, 1992), p. 233.
[56] S. R. Kulkarni et al., Nature (1998) (astro-ph/9807001) (in press).
[57] K. Iwamoto et al., Nature (1998) (astro-ph/9806382) (in press).
[58] L. Wang and J. G. Wheeler, Astrophys. J. (1998) (astro-ph/9806212) (submitted).
[59] J. S. Bloom et al., Astrophys. J. (1998) (astro-ph/9807050) (submitted).
[60] J. P. Norris, J. T. Bonnell, and K. Watanabe 1998, Astrophys. J. (1998) (astro-ph/9807322) (submitted).
[61] G. Amelino-Camelia et al., Nature 393, p. 763 (1998).